ELSEVIER

17 July 2000

Physics Letters A 272 (2000) 86–92

PHYSICS LETTERS A

www.elsevier.nl/locate/pla

Visible-range spectroscopy and a lifetime measurement on Kr^{22+} in an electron beam ion trap

E. Träbert *, S.B. Utter, P. Beiersdorfer

Department of Physics and Space Technology, Lawrence Livermore National Laboratory, Livermore, CA 94551, USA

Received 8 March 2000; received in revised form 4 May 2000; accepted 29 May 2000
Communicated by B. Fricke

Abstract

The $3s^2 3p^2\ ^3P_1 - ^3P_2$ transition in the Si-like ion Kr^{22+} has been studied using an electron beam ion trap (EBIT). A new wavelength value, (384.14 ± 0.02) nm, results from employing a novel spectrometer system that combines high speed and higher spectral resolution than applied before. The spectral resolution is high enough to observe source broadening. A new lifetime measurement [(6.82 ± 0.1) ms] differs from previous results (including our own) and now corroborates semiempirically scaled calculations.

PACS: 32.70.Cs; 32.30.Rj; 39.90.+d

1. Introduction

Electric-dipole forbidden transitions between the fine structure levels of the ground configuration of highly-charged ions are well established tools of plasma diagnostics, indicating the presence of specific charge states and thus of elemental species and rough range of plasma temperature [1,2]. For example, the identification of some of the solar coronal lines with fine structure transitions in highly-charged ions revealed that the corona is much hotter than the underlying photosphere. We are engaged in a series of experiments that aim at improving the knowledge on such transitions, for wavelengths and transition rates, by using an electron beam ion trap (EBIT). As a test case for the study of technical problems and new equipment, we have chosen the transition $3s^2 3p^2\ ^3P_1 - ^3P_2$ in the Si-like ion Kr^{22+} which under appropriate running conditions of EBIT gives rise to the most intense line in the visible Kr spectrum. The line has been observed in a tokamak fusion test plasma before, at a wavelength of (384.09 ± 0.03) nm [3,4]. Its transition rate has been measured twice before, both times using an EBIT [5,6]. However, all earlier EBIT lifetime measurements on transitions in the visible spectral range [5–7] remained notably less precise than corresponding measurements in the X-ray range that count among the most precise atomic lifetime measurements available on few-electron ions [8,9]. The preceding experiment on Kr at NIST Gaithersburg [5], for example, suffered from a considerable scatter of the results of individual data runs

* Corresponding author. Permanent address: Fakultät für Physik und Astronomie, Ruhr-Universität Bochum, D-44780 Bochum, Germany. Tel.: +49-234-700-7310; fax: +49-234-709-4172.
E-mail address: traebert@ep3.ruhr-uni-bochum.de (E. Träbert).

0375-9601/00/$ - see front matter
PII: S0375-9601(00)00397-2

and was quoted with an 8% lifetime error estimate, while the preceding LLNL experiment [6] reached an uncertainty of 5% (estimated from intrinsic factors), but was suspected of possible systematic error due to a measurement with only poor spectral resolution (using a prism spectrometer without exit slit).

The new experiment aimed at both a better spectral resolution and a much higher signal-to-noise ratio. For this goal, the new EBIT experiments started out with a novel transmission grating spectrometer [10] that promised both higher speed and much higher spectral resolution than were available before. For the atomic lifetime measurement, a new high-transmission imaging system was constructed that promised data rates leading to much better statistical reliability than had been achieved in earlier experiments, and also much better spectral resolution than in the preceding broad-band prism spectrometer measurement [6].

2. EBIT

The electron beam ion trap (EBIT) [11] is a room-size device that provides low-kinetic energy ions of any charge state [12]. This compares favourably with the one other known such device that produces such highly charged ions, the much larger heavy-ion accelerator. Key to the study of many physics topics treated with EBIT is precision spectroscopy, from the X-ray range to the visible. Due to the absence of Doppler shifts, this is more straightforwardly achieved at EBIT than at fast ion beams.

EBIT has demonstrated that its low particle density ($\leq 10^9$ atoms/cm^3) permits the appearance of radiative decays from levels with many-ms lifetimes and, thus, the study of magnetic dipole (M1) transitions between fine structure levels in ions as highly charged as Au^{57+} [6]. In fact, such M1 transitions in somewhat lower-charge state ions tend to dominate the visible spectra of Ar, Kr and Xe that have been recorded at EBIT [6,13,14]. However, the wavelengths of these forbidden lines are difficult to predict precisely, and experiment would have to identify single lines in a correspondingly wide wavelength range. Therefore experiment needs a number of other parameters beyond the wavelength prediction to identify individual forbidden transitions.

By varying the energy of the electron beam in EBIT, production thresholds for individual lines can be established that help line identification. For example, using a low-resolution prism spectrometer, Crespo et al. [14] have studied Kr and found a number of strong lines in the wavelength range 380–640 nm that are assumed to arise from M1 transitions. By their appearance thresholds, these lines are associated with Si- to V-like ions of Kr (384 nm Si-like, 403 nm Ar-like, 450 nm Ca-like, 520 nm Ti-like or V-like, 521 nm Ca-like, 541 nm K-like, 545/546 nm Ca-like, 551 nm Ca-like, 579 nm Ar-like, 637 nm K-like), but only for some of the lines has an actual classification been achieved [14].

Last, but not least, the experience gained in our X-ray lifetime measurements indicates that a proper choice of EBIT running conditions might be crucial for clean lifetime data, too [9,15]. The present measurements have been done on Livermore's EBIT-2, which for most practical purposes in the present context has parameters similar to SuperEBIT in the same laboratory (used in the precursor work [6]), but has a slightly higher gas load and thus slightly poorer vacuum. In none of the present EBITs the pressure in the very trap volume can be measured directly (only in the adjacent wider spaces that are not quite as well cooled by the liquid He. However, charge exchange measurements (ion survival measurements) revealed a notable difference in collisional loss rates of ions in both devices.

3. Spectroscopic measurement

The Lawrence Livermore National Laboratory (LLNL) EBIT laboratory has the most experience and the most extensive spectroscopic equipment, so that systematic studies are most feasible here. Recently, a transmission grating spectrometer with an extremely high diffraction efficiency grating (up to about 90% into a single diffraction order, for wavelengths near 360 nm) [16] and consequently a high throughput was constructed at LLNL that at the same time delivers much higher resolution than many other spectrometers of similar size, with line widths down to 0.1 nm (for our slitless operation on EBIT). This

instrument images the narrow elongated ion cloud in EBIT onto the detector without any mechanical entrance slit, thus using the available light optimally. The ion cloud is mostly defined in width by the 70 μm diameter electron beam [17]. A translatable CCD camera with a 25 mm wide active region permits the recording of overlapping spectra of about 10 nm spectral width in the vicinity of the Kr line of interest (Fig. 1). EBIT operating conditions were varied, such as varying the electron beam energy below and above threshold for the ion of interest, and setting the middle drift tube potential so that trapping was either allowed or prevented. For our charge state of presently primary interest, (Kr^{22+}), the production threshold is near 1 keV electron energy, and the optimum production is near 1.4 keV. At higher electron beam energies than these, higher charge state ions are produced, and $q = 22+$ becomes a minority and then transient charge state in the ionization chain. However, with a steady electron beam and a continuous Kr gas influx, the strongest Kr^{22+} line in the EBIT spectrum persists up to electron energies of many keV. The electron beam current reached 100 mA to 160 mA for electron energies of several keV, whereas at lower electron energies the attainable current (and thus the signal) is lower.

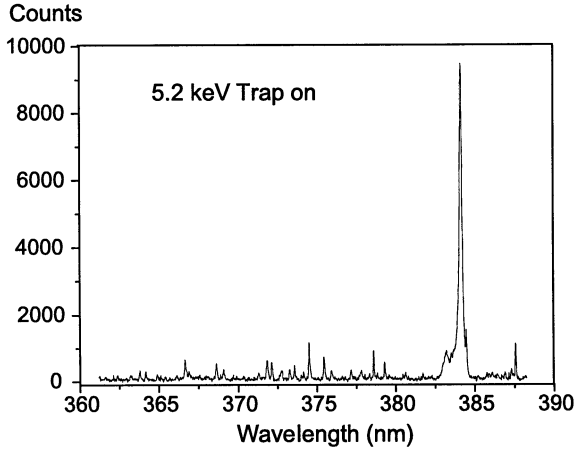

Fig. 1. Survey spectrum of Kr, with the Kr^{22+} line at full scale. At 5.2 keV, the electron beam energy is far above the 1 keV production threshold for Kr^{22+}. The continuum at the foot of the line (discussed in the text) is present also in spectra at 1.35 keV, but has a somewhat different shape.

During injection of Ne or Kr, quite a number of weak spectral lines showed up in spectra recorded with or without actual ion trapping. Their small width confirmed the good spectral resolution ($\lambda/\Delta\lambda \geq 5000$) of the spectrometer. Their presence under both conditions reveals that they relate to low charge state ions of elements Ne or Kr streaming through the gas injector into the EBIT chamber, reaching the radiating charge state by collisions with the electrons in the beam but without the need to be trapped (see also [18]). The decisive wavelength reference data [19] are for lines that are known with high wavelength precision since the 1930s, but many of which have defied detailed assignment beyond elemental species and (possibly) charge state ever since.

In our range of study, 365 nm to 404 nm, five spectral lines showed only when the voltages applied to the drift tubes permitted trapping. This suggests an association of these lines with transitions in higher-charge state ions. For four of the lines (366.66 nm, 378.59 nm, 379.28 nm, 384.14 nm (Kr^{22+})) wavelengths have been determined to ± 0.02 nm. For the line at 402.69 nm (Kr^{18+} [14]) there is no new wavelength determination yet because of the intricacy of the necessary wavelength calibration. The first three of the above lines are only a little broadened beyond the line width of the reference lines (linewidth FWHM$\approx$ 0.07 nm versus 0.04 nm). This may either indicate a relatively low charge state or a short atomic lifetime that lets the ions radiate before they leave the trap volume. The latter two lines, however, which are known to originate from high charge state ions, are massively broadened (FWHM $\approx$ 0.15 nm). Several of the narrow background lines appear close to or even within the much wider line profile of the strong Kr^{22+} line (see Fig. 2).

Measurements show that the ion temperature ranges from 0.5 to 1.5 keV for the trapping conditions of the present experiment [20]. At 1 keV ion energy, the Doppler line width (FWHM) for Kr ions is of order 0.08 nm. Obviously, our reference lines are from ions of much lower energy, as their emission lines are narrower. Explaining the full line width of the highly-charged ions by Doppler broadening would require an ion energy of order 4 keV, which is not likely. Instead, we consider much of this line broadening to reflect the source size. This source size apparently is different for ions of differ-

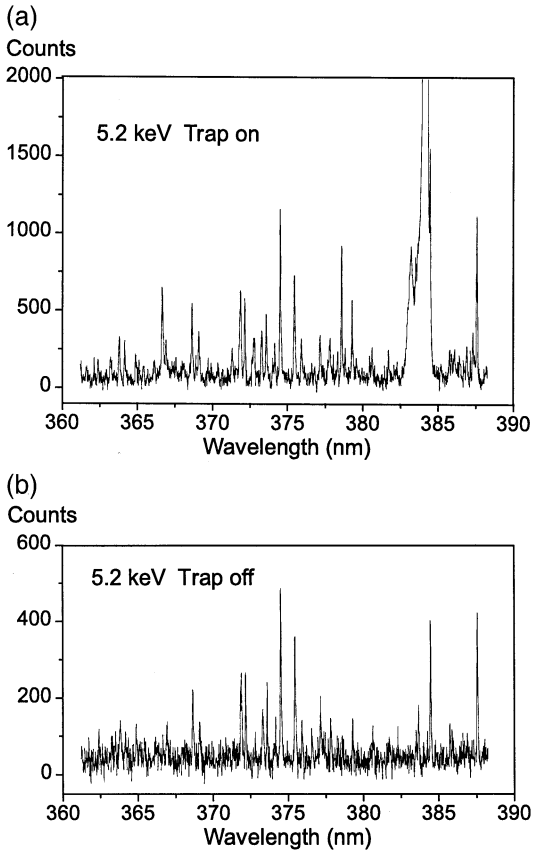

Fig. 2. Spectra of Kr in the same range as in Fig. 1, but with a signal scale expanded in order to enhance the spectral features of lower intensity. (a) Electron energy 5.2 keV, trap on; (b) electron energy 5.2 keV, trap off.

ent charge state, and it relates to the production and trapping mechanism. Axial confinement in the trap is achieved by drift tubes at different potentials: more highly-charged ions experience higher potential walls (proportional to eqU, with elementary charge e, charge state q and potential difference U) and consequently are better trapped axially. This axial potential resembles a square well, and all ions are confined to about the same trap length. Radial trapping, in contrast, is achieved by the electron beam, the potential of which is falling off radially ('soft potential'). The radial confinement is assisted by the strong magnetic field that suppresses a flow of charged particles across the field lines.

The observation of significantly broadened spectral lines from highly charged ions implies that some of the ions, after so many ionizing collisions, are energetic enough to gyrate notably out of the main trap region, that is, out of the volume reached by the electron beam. This behaviour affects the ionization balance, as for a major part of their orbit the ions are no longer exposed to the electrons that may effect both ionization and recombination. The ion heating effect underlying the source broadening has been noted before (see the review by Donets [21]), but our experiment visibly demonstrates the ion-cloud expansion effect that is caused by the higher thermal energy of highly charged trapped ions by means of optical spectroscopic observation and thus complements measurements performed with X-ray imaging methods [22,23].

Some of our highly resolved spectra showed another wide spectral structure adjacent to the Kr^{22+} line, on the short-wavelength side of the line of interest and merging with it. This wide, continuous structure appeared only under trapping conditions and only near the Kr line of interest, not with other bright lines. By a systematic electron beam energy variation it was ascertained that the 'continuum' showed exactly in coincidence with the strong Kr^{22+} line. This simultaneity hinted at a common origin of the line and its 'satellite', perhaps caused by a chance optical effect like internal reflection in the spectrometer that becomes visible only with the strongest line. While slight rotations of the spectrometer lenses around a vertical axis showed the appearance of imaging errors with increasing rotation angle, the 'satellite' line persisted. A similar rotation of the thin quartz plate that carries the grating structure, however, had a very specific new effect: Only in a very narrow angular range, apparently selected in the optimization during the setting-up process of the spectrometer, the image of the line of interest becomes particularly bright on the detector, and then also the 'satellite' rises above the ordinary weak lines and the background level. We cannot offer a detailed physical explanation of this effect, but we point out that the grating design is based on a specific geometry with 60° deflection to be achieved for the third harmonic of Nd:YAG laser light [16]. Our set-up, being only close to that geometry, but not working exactly at that particular wavelength, may suffer the appearance of a new version of a grating ghost as is known from reflective grating

spectroscopy. No such ghosts have been seen of the weaker lines. However, at the same intensity ratio they would likely be hidden in the background noise. By the way, the Kr^{22+} line remains the strongest line in the visible EBIT spectrum of Kr even when avoiding this ghost effect. However, as the shape of the line when using the transmission grating spectrometer may be slightly distorted, as well as there are foreign lines within the line profile, this limits the precision with which the wavelength of the line of interest can be determined.

4. Decay curve measurements

CCD cameras, as employed in the transmission-grating spectrometer, are not suited to time-resolved operation in the sub-second cycling mode of EBIT lifetime measurements because of their long read-out times. Instead, a regular low-noise photomultiplier (Hamamatsu type R2557, 1/2'' diameter, end-on cathode, 401K spectral sensitivity curve) was used in combination with an optical bandpass filter (mean wavelength 385 nm, band pass 5 nm). Optical coupling of the ion trap volume to the photomultiplier was by two $f/4$ lenses of 10 cm diameter, positioning the detector more than 1 m away from EBIT and its associated magnetic fields. The trap was run in a cycling mode; within about 0.1 s the ion cloud was established, as could be seen from the saturation of the optical signal. Then the electron gun anode and beam acceleration voltages were switched off within less than 0.1 ms, and the decay was observed for an interval of 50 ms to 80 ms, which is a high multiple of the expected atomic lifetime. The ion production and optical decay cycle ran at a frequency of about 5 Hz; every about 5 s the ion cloud was dumped from the trap in order to counteract the usual accumulation of heavy-ion contaminants.

The detector signal pulses were time stamped and collected by a multi-channel event mode system synchronized to the EBIT timing pattern. The time base was established by a free-running 100 kHz frequency generator. The time stamp represented the number of pulses of this generator between the reference pulse and the photon signal; the 10 μs jitter of individual time stamps introduced by the non-synchronized oscillator is unimportant for the present 6.8 ms lifetime that is determined from several hundred data points (grouped in time bins of 0.1 ms), each of which represents a multitude of signal events.

In a companion study on Ar [24], the gas injection pressure was varied in three steps by an order of magnitude. Gas injection, however, is only one of the components of the gas load in EBIT, and thus the actual pressure change in the trap volume (where direct pressure measurements are not feasible at any of the present EBITs) will be much less. To within the statistical scatter of the lifetime results, no dependence of the optical lifetime was found. For the present lifetime experiment on Kr, an injection pressure in the middle of the tested range was used.

The middle drift tube voltage was kept 200 V more negative than the outer drift tubes. The electron energy was varied in several steps from about 1 keV (just below the apparent production threshold) to 1.4 keV. At 1050 to 1100 eV, the signal rate was markedly lower than at electron beam energies of 1200, 1300 or 1400 eV. This has two reasons: At the higher of these energies, the electron beam current (38 to 52 mA) was somewhat higher than at the lower ones (29 to 35 mA). Also, the production cross section for the desired charge state usually peaks at an energy of a few hundred eV above threshold. While charge states $q = 25+$ and $26+$ might appear at the higher electron energy, they are still far below their production optimum, and their appearance in the charge state distribution is accompanied by a reduction of the fractions of lower charge states.

Not only the data rate was low for the runs just above excitation threshold, but also the apparent lifetime extracted from two curves recorded at an electron beam energy of 1100 eV was slightly (by a few percent) shorter than obtained from three (statistically much more significant) curves recorded at electron beam energies of 1200 to 1400 eV. This variation may result from the presence of spectral blends, even as they are weak (Fig. 1), as they must be (relatively) more important just above the excitation threshold of the Kr^{22+} line. The total signal accumulated (above background) exceeded 10^5 counts, which limits the uncertainty of the mean of the present lifetime data to about 0.3%. A sample curve is shown in Fig. 3. Charge exchange rate measurements [20] performed in EBIT-2 close in date to the present experiments indicate storage time constants of just below 1 s. Correspondingly we

correct our raw lifetime result (from the three data runs at 1200 eV to 1400 eV) of 6.75 ms by 1% and add half of this systematic error to the uncertainty budget. This uncertainty covers also a possible level repopulation after recombination of more highly charged ions, since under our running conditions the charge state of interest is one of the highest present, and more highly charged ions are much less abundant to start with. The time constants of such processes would be close to what we measure as charge exchange rates.

However, the individual data sets yielded fit results that scattered by more than the (small, below 1%) statistical uncertainties, indicating the possible presence of further unidentified systematic errors at the 1% level. We combined the listed errors in quadrature. Thus the data sample permitted us to determine a lifetime value of the Kr^{22+} $3s^2 3p^2\ ^3P_2$ level of (6.82 ± 0.1) ms. This is clearly more precise than the earlier data [5,6] and differs from our previous result by about 1.5 of the earlier (larger) error estimate (Table 1). This trend corroborates the assumption of unevaluated systematic errors in the earlier work, as was suspected on the evidence of unexplicable data scatter in the NIST work [5] (some of the individual lifetime results overlapped with the present results) and the evident and discussed spectral blending problem in our earlier LLNL study [6]. Two available lifetime predictions have been obtained by Biémont and Bromage [25] using a HXR (Hartree–Fock with statistical exchange and relativistic corrections) code and by Huang [26] who used a fully relativistic MCDF (multi-configuration Dirac–Fock) code. Neither calculation reproduces the experimental energy interval in question, which enters the calculation of the transition rate by the third power, and therefore both require a semiempirical correction for this shortcoming. The corrected results are reasonably close to our present experimental lifetime result (Table 1). Kaufman and Sugar [4] also list the transition rate. They refer to the line strengths calculated by Huang, but possibly use their own estimated transition wavelength and thus arrive at a slightly different prediction from our conversion result. We have meanwhile been informed by Dr. J.M. Vilkas that he is undertaking a fresh calculation of the transition rate of this transition in the Si isoelectronic sequence.

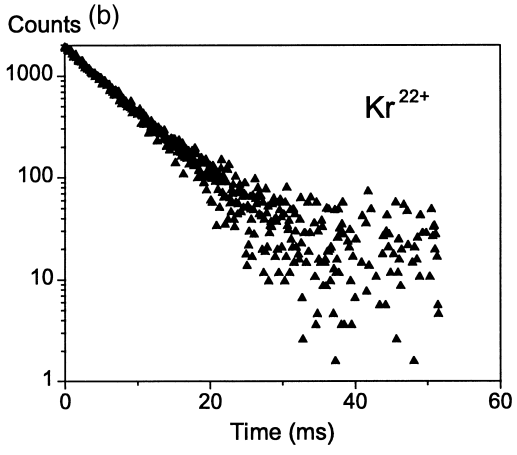

Fig. 3. Decay curve obtained at the position of the Kr^{22+} $3s^2 3p^2\ ^3P_1 - ^3P_2$ transition. Electron beam energy 1.2 keV. While the optical signal is monitored all the way through the trapping cycle, only the decay part during the time when the electron beam is shut off is shown, after subtracting a background of 600 counts per channel.

Table 1
Radiative lifetime values (ms) for the Kr^{22+} $3s^2 3p^2\ ^3P_2$ level. Calculation (raw) and (mod.) refer to theoretical data before and after modification for experimental term differences

	Calculation (raw)		Calculation (mod.)
Theory	6.46	[25]	6.78
	5.83	[26]	6.69
	6.85	[4]	
Experiment	5.7 ± 0.5	[5]	
	6.3 ± 0.3	[6]	
	6.82 ± 0.1	This work	

5. Conclusion

The present measurement has obtained an accurate wavelength value for a transition in the ground state complex of Kr^{22+}. The line of interest appears clearly broadened, and we see narrow reference lines from low-charge state ions superimposed on the line profile. Thus high-resolution spectroscopy has been shown to yield a new handle at finding out which line in an optical EBIT spectrum originates from long-lived levels, by the associated source broadening. However, the interpretational problem of the exact shape of the broadened Kr^{22+} line is related to

peculiarities of the newly employed transmission grating spectrometer and does not yet permit the extraction of a much improved wavelength value.

Our EBIT operation and data evaluation techniques, including the measurement of ion storage times (against losses due to charge exchange), has been corroborated by good agreement of X-ray lifetime measurements [8,9] with reliable predictions for He-like ions. From our systematic tests we deduce that our measurement of the radiative transition rates in the visible spectral range, here of a prominent line in Kr^{22+}, is significantly more accurate than the earlier attempts [5,6] and now produces a value that is substantially different from those. Agreement with theory is reasonable after semiempirical correction of the latter for the transition energy. We presently see no room for a further shift of the experimental lifetime results for Kr^{22+} that would be due to unrecognized systematic errors exceeding our present error estimate. An eventual further improvement of the precision, however, may well become possible after reaching a better understanding of the ion dynamics and charge exchange processes in EBIT. The presently achieved lifetime precision of 1.5% already exceeds the precision required for most applications, but is appropriate to improve the error budgets in various applications and to calibrate calculations.

Acknowledgements

We appreciate the help of G.V. Brown, H. Chen and P.A. Neill with the EBIT runs and experiments. The work has been performed at LLNL under the auspices of the USDoE under contract No. W-7405-ENG-48. E.T. gratefully acknowledges travel support from the German Research Association (DFG), as well as the hospitality experienced in the LLNL EBIT group. We thank a referee for pointing out that R.W. Schmieder discussed thermal ion cloud expansion in EBIS, a device that is closely related to EBIT, in a Sandia National Laboratories report SNLL 8347 (1987) that we were unable to obtain.

References

[1] M. Eidelsberg, F. Crifo-Magnant, C.J. Zeippen, Astron. Astrophys. Suppl. Ser. 43 (1981) 455.
[2] B. Edlén, Phys. Scr. T 8 (1984) 5.
[3] J.R. Roberts, T.L. Pittman, J. Sugar, V. Kaufman, W.L. Rowan, unpublished work (1985), quoted in [4].
[4] V. Kaufman, J. Sugar, J. Phys. Chem. Ref. Data 15 (1986) 321.
[5] F.G. Serpa, J.D. Gillaspy, E. Träbert, J. Phys. B: At. Mol Opt. Phys. 31 (1998) 3345.
[6] E. Träbert, P. Beiersdorfer, S.B. Utter, J.R. Crespo López-Urrutia, Phys. Scr. 58 (1998) 599.
[7] F.G. Serpa, C.A. Morgan, E.S. Meyer, J.D. Gillaspy, E. Träbert, D.A. Church, E. Takács, Phys. Rev. A 55 (1997) 4196.
[8] J.R. Crespo López-Urrutia, P. Beiersdorfer, D.W. Savin, K. Widmann, Phys. Rev. A 57 (1998) 238.
[9] E. Träbert, P. Beiersdorfer, G.V. Brown, A.J. Smith, S.B. Utter, M.F. Gu, D.W. Savin, Phys. Rev. A 60 (1999) 2034.
[10] S.B. Utter, P. Beiersdorfer, J. Britten, R.S. Thoe, Rev. Sci. Instrum., in preparation.
[11] M.A. Levine, R.E. Marrs, J.R. Henderson, D.A. Knapp, M.B. Schneider, Phys. Scr. T 22 (1988) 157.
[12] R.E. Marrs, S.R. Elliott, D.A. Knapp, Phys. Rev. Lett. 72 (1994) 4082.
[13] F.G. Serpa, E.W. Bell, E.S. Meyer, J.D. Gillaspy, J.R. Roberts, Phys. Rev. A 55 (1997) 1832.
[14] J.R. Crespo López-Urrutia, P. Beiersdorfer, K. Widmann, V. Decaux, Phys. Scr. T 80 (1999) 448, and private communication.
[15] E. Träbert, P. Beiersdorfer, S.B. Utter, Phys. Scr. T 80 (1999) 450.
[16] H.T. Nguyen, B.W. Shore, S.J. Bryan, R.D. Boyd, M.D. Berry, Opt. Lett. 22 (1997) 142.
[17] S.B. Utter, P. Beiersdorfer, J.R. Crespo López-Urrutia, K. Widmann, Nucl. Instrum. Methods A 428 (1999) 276.
[18] S.B. Utter, P. Beiersdorfer, G.V. Brown, Phys. Rev. A 61 (2000) 030503.
[19] J. Reader, C.H. Corliss, in: CRC Handbook of Chemistry and Physics, 68th ed., Boca Raton: CRC Press, 1987, p. E-201.
[20] P. Beiersdorfer, R.E. Olson, L. Schweikhard, P. Liebisch, G.V. Brown, J.R. Crespo López-Urrutia, C.L. Harris, P.A. Neill, S.B. Utter, K. Widmann, AIP Conf. Proc. 500 (2000) 626.
[21] E.D. Donets, Rev. Sci. Instrum. 69 (1998) 614.
[22] M.B. Schneider, M.A. Levine, C.L. Bennett, J.R. Henderson, D.A. Knapp, R.E. Marrs, in: A. Hershcovitch (Ed.), Int. Symp. Electron Beam Ion Sources and Their Applications, Upton, NY, AIP Conf. Proc., vol. 188, Am. Inst. Phys., New York, 1988, p. 158.
[23] N. Nakamura, A.Ya. Faenov, T.A. Pikuz, E. Nojikawa, H. Shiraishi, F.J. Currell, S. Ohtani, Rev. Sci. Instrum. 70 (1999) 1658.
[24] E. Träbert, P. Beiersdorfer, S.B. Utter, G.V. Brown, H. Chen, C.L. Harris, P.A. Neill, D.W. Savin, A.J. Smith, Astrophys. J., 2000, in print.
[25] E. Biémont, G.E. Bromage, Mon. Not. R. Astron. Soc. 205 (1983) 1085.
[26] K.-N. Huang, At. Data Nucl. Data Tables 32 (1985) 503.